Crystal-field effects in the diffusion of transition-metal ions in silver chloride

A. P. Batra

Department of Physics and Astronomy, Howard University, Washington, D.C. 20059

J. P. Hernandez and L. M. Slifkin

Department of Physics and Astronomy, University of North Carolina, Chapel Hill, North Carolina 27514

The diffusion in silver chloride of divalent vanadium, chromium, iron, cobalt, and nickel is shown to occur by means of vacancies. The high-temperature activation energy for diffusion of these first transition row solutes in AgCl is found to vary systematically with atomic number, dropping from 2.08 eV for V^{2+} to 1.18 eV for Mn^{2+} and then rising again to 1.88 eV for Ni^{2+}. This variation can be quantitatively accounted for by the effect of the crystalline electric field on the d electrons during the solute-vacancy interchange.

INTRODUCTION

A large number of cations diffuse in silver halides by means of vacancies. The only known exceptions are the monovalent noble-metal ions, which diffuse in large part interstitially. These latter ions are only singly charged and have a filled outer d shell; for them an interstitial site becomes favorable because of a strong covalent interaction between the solute and the neighboring tetrahedron of halide ions.

The charge of the solute ion is known to significantly influence impurity ion diffusion in a crystal. In fact, in cubic metals, particularly the noble metals, much of the diffusion data have successfully been interpreted by a screened-interaction model proposed by Lazarus.[1,2] Our understanding, on the other hand, of solute diffusion in even the simplest ionic crystals is far from satisfactory.[3]

In ionic materials, recent experiments indicate that the ion transport is also affected by the details of the electronic structure of the solute ion. From studies of dielectric loss in doped alkali halides, Varotsos and Miliotis[4] found qualitative differences between the behavior of ions with inert gas cores and those with outer d electrons. For ions with no d electrons, they report that the activation energy (which here refers to the jump of the vacancy *around* the solute ion) increases linearly with solute ion radius. On the other hand, for ions with an outer d shell, this energy was found to be essentially independent of solute radius. Also, the partitioning of transition elements in duplex scales on oxidized alloys has been related to the difference in stabilization energies for octahedral and tetrahedral sites, as estimated from crystal-field theory.[5]

More recently, we have quantitatively demonstrated the role of electronic structure in the mobility of solute ions in an ionic crystal by mea-suring the tracer diffusion of a set of consecutive divalent transition-metal ions in AgCl. A brief summary of the results has already appeared.[6] The present paper now gives a detailed account of this investigation, and also includes some additional findings.

EXPERIMENTAL

The standard tracer, thin-layer, sectioning technique was employed for all diffusion measurements. The single crystals of pure silver chloride used in these experiments, kindly provided by Mr. C. B. Childs, contained no more than one part per million of divalent cation impurity. Each diffusion run was made on a carefully prepared and thoroughly annealed virgin specimen.

The tracers, $^{48}VOCl_2$ (carrier free), $^{51}CrCl_3$ (758 Ci/g), $^{59}FeCl_3$ (30 Ci/g), $^{58}CoCl_2$ (carrier free), and $^{63}NiCl_2$ (18 Ci/g), were obtained from the International Chemical and Nuclear Corporation. A microcurie or less of the appropriate tracer was applied to a prepared broad, flat surface of the specimen, which was then encapsulated for diffusion anneal under a partial pressure of either electronic grade hydrogen chloride gas (for most of the runs) or else ultrapure helium plus chlorine (for some of the early runs). The hydrogen chloride atmosphere was found to be quite effective in eliminating any surface hold-up of the tracer, which otherwise presumably resulted from formation of a metal oxide or oxychloride. This HCl atmosphere was particularly important for the iron tracer for which substantial surface hold-up otherwise occurred (even in an ambient chlorine pressure of 0.5 torr), and for the vanadium tracer, for which no tracer penetration is observed in $He:Cl_2$ because of the stability of $VOCl_2$. The diffusion anneal, sectioning, and weighing of sections followed the procedures previously described elsewhere.[7]

In the case of ^{48}V, ^{51}Cr, ^{59}Fe, and ^{58}Co tracers, the radioactivity in each section was assayed by counting the total γ radiation above a certain low bias, with a well-type scintillation counter. However, the ^{63}Ni tracer emits only β radiation that is so weak (67 keV) as to be appreciably absorbed in the 5×10^{-4} cm thick AgCl section; hence, in this case, the radioactivity as a function of depth was assayed by counting the residual activity at the surface of the specimen after each section was taken. An accurately reproducible geometry was in this case insured by mounting the thin-window Geiger-Müller tube onto the microtome so that the specimen could be located in an exactly reproducible position beneath the counter window after each sectioning step.

RESULTS

As with more conventional section procedures used for ^{48}V, ^{51}Cr, ^{59}Fe, and ^{58}Co tracers, a Gaussian tracer distribution in the specimen after diffusion is also expected from the surface counting technique employed for ^{63}Ni, because of the high absorption coefficient of its β radiation. Several typical penetration plots are shown in Figs. 1 and 2 and give a fair indication of the quality of data. From such plots, the diffusion coefficients for these tracers were calculated in the usual manner, and are given in Table I together with the corresponding annealing temperatures and times. The overall error in each D, including that due to error in the measurement of the diffusion temperature, is estimated to be no more than 5%. Figures 3–5, which also include for comparison the results of some other recent investigations on diffusion of iron and cobalt in AgCl, show the
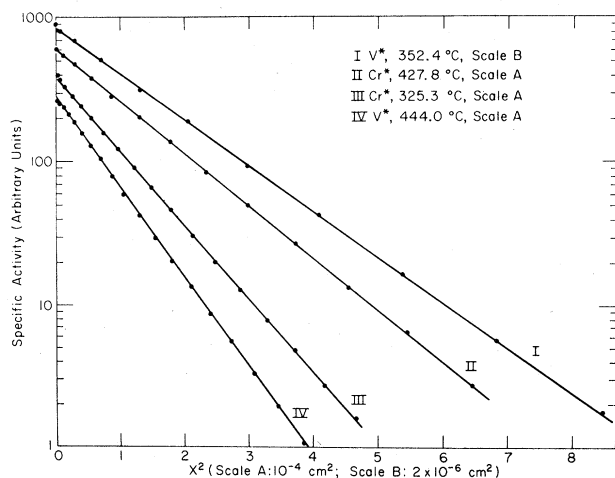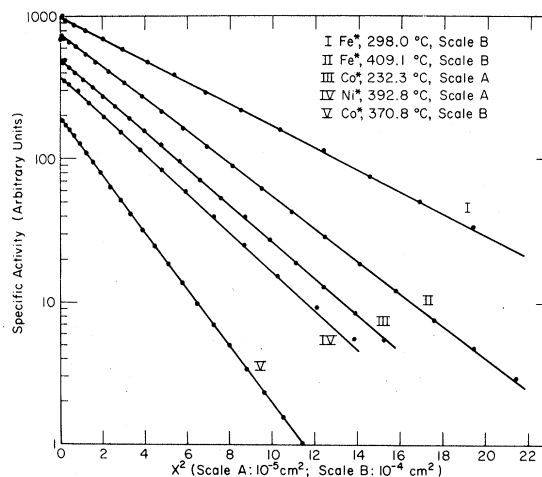
FIG. 2. Typical penetration plots for the diffusion of Fe^{2+}, Co^{2+}, and Ni^{2+} in pure AgCl.

logarithms of the diffusion coefficients of the five tracers plotted as a function of reciprocal temperature. These results are discussed in more detail below.

Diffusion of vanadium

Excellent vanadium-tracer penetration profiles which accurately checked with the Gaussian solution for the thin-film boundary condition were obtained over the temperature range 352–445 °C when the diffusion anneals were carried out in hydrogen chloride atmosphere. The replacement of O^{2-} ion in the surface deposit of $VOCl_2$ by two Cl^- ions should still leave vanadium as a quadrivalent ion (rare-gas configuration); it is, however, not likely that this is the valence state in which it diffuses in AgCl. Whereas vanadium enters such quadrivalent compounds as TiO_2 and CeO_2 in the form of V^{4+}, EPR[8] and optical-absorption studies[9] in AgCl indicate that in this case an Ag^+ ion at a normal site is replaced instead by V^{2+}. This decrease in solute charge is presumably in order to decrease the necessary formation energy of charge-compensating defects. Furthermore, the existence of V^{2+}-cation vacancy complexes in AgCl has also been inferred from thermal depolarization (ITC) studies.[10] Thus, it is reasonable to assume that vanadium diffuses as V^{2+} in AgCl. Moreover, this reduction of solute valence is consistent with earlier experiments on tracers of copper and gold in AgCl, where even though the solutes were applied in a state of higher valence (Cu^{2+} and Au^{3+}), the diffusion behavior was that of monovalent ions (unless the ambient chlorine pressure was very high).[11,12]

The Arrhenius line (Fig. 3), fitted by least

FIG. 1. Typical penetration plots for the diffusion of V^{2+} and Cr^{2+} in pure AgCl.

TABLE I. Diffusion of vanadium, chromium, iron, cobalt, and nickel in pure AgCl.

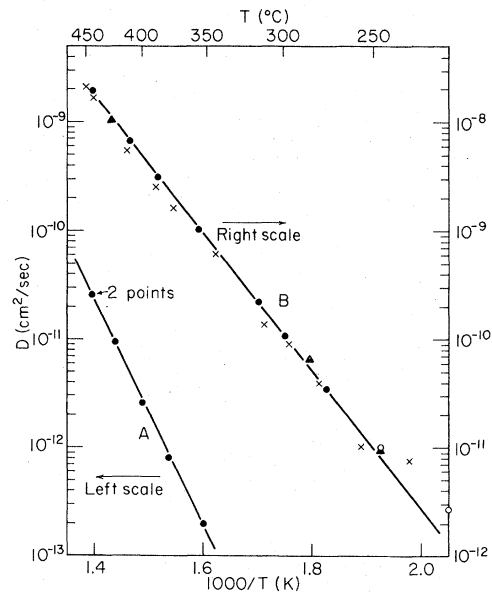| Tracer	Temperature (°C)	Time (sec)	Diffusion coefficient (cm²/sec)
^{48}V	444.0	6.84×10^5	2.54×10^{-11}
	444.0	1.80×10^5	2.50×10^{-11}
	422.7	7.79×10^5	9.47×10^{-12}
	399.5	1.38×10^6	2.53×10^{-12}
	378.9	3.11×10^6	7.99×10^{-13}
	352.4	3.11×10^6	1.94×10^{-13}
^{51}Cr	439.5	1.44×10^4	3.16×10^{-9}
	427.8	1.44×10^4	2.11×10^{-9}
	401.3	4.46×10^4	8.99×10^{-10}
	375.0	1.01×10^5	3.76×10^{-10}
	350.6	1.21×10^5	1.63×10^{-10}
	325.3	3.28×10^5	6.41×10^{-11}
^{59}Fe	442.0	1.44×10^4	1.99×10^{-8}
	409.1	1.44×10^4	6.69×10^{-9}
	408.9	2.07×10^4	6.65×10^{-9}
	385.9	6.76×10^4	3.05×10^{-9}
	354.5	8.59×10^4	1.02×10^{-9}
	314.2	1.71×10^5	2.19×10^{-10}
	298.0	1.34×10^6	1.06×10^{-10}
	274.3	6.53×10^5	3.51×10^{-11}
^{58}Co	441.1	1.23×10^4	2.10×10^{-8}
	421.5	1.36×10^4	1.04×10^{-8}
	396.7	3.02×10^4	4.14×10^{-9}
	370.8	3.37×10^4	1.62×10^{-9}
	348.8	1.42×10^5	6.98×10^{-10}
	328.1	2.61×10^5	2.91×10^{-10}
	310.6	5.84×10^5	1.50×10^{-10}
	293.0	6.26×10^5	7.04×10^{-11}
	269.0	1.19×10^6	2.42×10^{-11}
	249.9	1.59×10^6	1.07×10^{-11}
	232.3	1.78×10^6	4.77×10^{-12}
	206.9	4.29×10^6	1.17×10^{-12}
^{63}Ni	440.5	2.12×10^4	2.21×10^{-9}
	416.4	2.13×10^4	7.60×10^{-10}
	392.8	3.33×10^4	2.47×10^{-10}
	373.8	8.15×10^4	1.25×10^{-10}
	350.2	1.71×10^5	4.27×10^{-11}

FIG. 3. (A) Diffusion coefficient of V^{2+} in AgCl as a function of temperature. (B) Diffusion coefficient of Fe^{2+} in AgCl, as a function of temperature. The solid circles refer to our data taken with an atmosphere of hydrogen chloride during the anneal and represent intrinsic diffusion; the open circles refer to diffusivities calculated from the "limiting" slopes of the non-Gaussian penetration plots obtained at the lowest temperatures. Solid triangles refer to our data taken with an atmosphere of chlorine plus helium; the crosses refer to data obtained by Foster and Laskar (Ref. 14) using a chlorine atmosphere.

squares to the data, corresponds to an activation energy of 2.08 eV and a preexponential factor of 1.1×10^4 cm² sec⁻¹. We have yet to understand the significance of the extremely large value of D_0 (also, as cited below, displayed by the nickel ion). The activation energy, however, does indicate a vacancy mechanism for vanadium diffusion in AgCl. Any interstitial contribution is definitely ruled out by the very small diffusion coefficients.

Diffusion of chromium

An activation energy of 1.25 eV and a preexponential factor of 2.0 cm² sec⁻¹ for diffusion of chromium in AgCl are deduced from the results of six successful diffusion runs (Fig. 4; solid

squares) in the temperature range 325–440 °C. These values also are indicative of solute migration by a vacancy mechanism.

The large and erratic scatter in the diffusion data below 325 °C (Fig. 4; open squares), obtained from the limiting slopes of somewhat non-Gaussian tracer penetration profiles, is perhaps a consequence of two competing sources of error—tracer hold-up at the specimen surface and nonradioactive contamination in the tracer solution.

Diffusion of manganese

The tracer diffusivity of ^{54}Mn in AgCl was reported in an earlier publication,[13] but because of its relevance to the present work, the main results are cited here. The Mn^{2+} was found to migrate by means of the vacancy mechanism, with an activation energy of 1.18 eV and $D_0 = 1.8$ cm² sec⁻¹.

Diffusion of iron

Those data on the diffusion of Fe^{2+} which are shown as solid circles in Fig. 3 pertain to diffu-
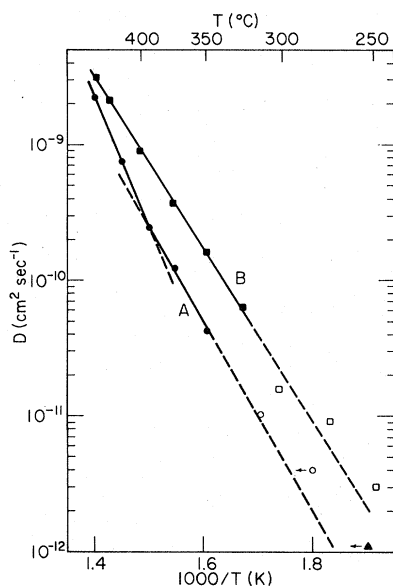
FIG. 4. (A) Diffusion coefficient of Ni^{2+} in AgCl, as a function of temperature. The solid circles refer to data characterizing intrinsic diffusion; open circles and the triangle refer to data obtained at lower temperatures from penetration plots which were visibly perturbed by the tracer impurities. (B) Diffusion coefficient of Cr^{2+} in AgCl, as a function of temperature. The solid squares represent data characterizing intrinsic diffusion; open squares refer to data obtained at lower temperatures from penetration plots which are visibly perturbed by the tracer contamination and tracer hold-up at the specimen surface.

sion anneals in hydrogen chloride gas, for which good Gaussian penetration profiles were obtained. Included in this figure are also the recent data of Foster and Laskar,[14] which lie consistently below our values (except for a point at the lowest temperature) and which often deviate from our results by as much as 30%, well outside the combined estimated limits of error. In those of our earlier diffusion anneals for which, instead of hydrogen chloride, we used an ambient low pressure of chlorine (plus helium as an inert buffer gas), there appeared an upward curvature in the initial portion of the penetration profile. This presumably resulted from the surface hold-up of tracer in the form of an iron oxide or oxychloride. In the absence of HCl, this blocking of the tracer was quite pronounced even at a temperature as high as 426 °C, which is just some thirty degrees below the melting point of AgCl. For these runs, the diffusion coefficients (Fig. 3, solid triangles) calculated from the long, deep Gaussian tails, however, agreed rather well with the unperturbed data later obtained with a hydrogen chloride atmosphere. Foster and Laskar consistently used

an ambient atmosphere of chlorine at low pressure, and all of their runs showed a considerable surface hold-up of tracer, which they attribute to a presumed very low solubility of iron in silver chloride, even at temperatures as high as 300 °C. We believe, however, that the tracer oxidation appears to be the most likely source of the perturbation of their penetration plots, and it may well be the cause of the lower diffusivities and the greater amount of scatter apparent in their results.

Although the present measurements on Fe^{2+} were carried out over the temperature range 215–442 °C, only the data above 270 °C appear to represent unperturbed intrinsic diffusion. These results can be expressed by an extremely well-defined activation energy of 1.26 eV and a preexponential factor of 14.2 $cm^2 sec^{-1}$. These parameters differ only slightly from the 1.27 eV and 15.1 $cm^2 sec^{-1}$ reported by Foster and Laskar and are definitely characteristic of solute migration by means of cation lattice vacancies.

In a diffusion run at 250 °C, not included in Table I or Fig. 3, the effect on the penetration plot of nonradioactive polyvalent cationic impurities present in the "high-specific-activity" tracer was quite noticeable: The tracer concentration versus depth fell off more rapidly than a Gaussian (in addition, a small upturn attributable to tracer hold-up was also observed in the near-surface region). Similar non-Gaussian penetration plots have also been observed earlier by Mitchell and Lazarus[15] for diffusion of a "dirty" tracer into a monovalent ionic crystal, NaCl. Such a curvature in the penetration plot does, in fact, provide a rather strong support in favor of migration by a vacancy mechanism. Further, the real tracer diffusion coefficients at these low temperatures could also perhaps be sensitive to crystal dislocations which—because of their electric charge and concomitant space charge regions—could exert a larger effect on diffusion in ionic crystals than in metals (this would be expected if, at the temperature of diffusion, the dislocations were positively charged). Both of these perturbing factors, tracer contamination and dislocation effects, would tend to raise the apparent diffusivity above its true value.

In order to minimize the influence of tracer contamination, the low-temperature data shown in Fig. 3 (open circles) were, therefore, obtained with the use of an extremely small amount (about 0.02 μCi) of tracer. The resulting penetration profiles were now only slightly curved, but the curvature in the near-surface region could conceivably have been partially masked by the opposite effect of some tracer hold-up at the surface. The two diffusion coefficients obtained at these

temperatures lie above the extrapolation of the high-temperature data, and each presumably represents only an upper limit. Nevertheless, these low-temperature experiments do, by virtue of the sign of the deviations, further corroborate the vacancy mechanism of diffusion. Thus it can be safely assumed that the iron tracer diffuses substitutionally in AgCl, at least down to 215 °C.

Diffusion of cobalt

The diffusion of cobalt in AgCl was measured over the temperature range 206–442 °C. Figure 5 shows that for the high-temperature regime, good agreement exists between our data and those of Blackwell,[16] but here also considerable differences appear at lower temperatures, presumably because of the sensitivity of the measurements to such extrinsic factors as discussed above. It would also seem almost certain that the ^{60}Co data of Murin et al.,[17] also shown in Fig. 5, do not characterize the intrinsic diffusion at all. The very low values of their diffusion coefficients could perhaps have resulted from utilizing only the initial portion of penetration plots obtained under conditions of a rather large oxide-induced tracer hold-up at the surface, which incidentally was also present to a small extent in Blackwell's plots.

As is evident from Fig. 5, the Arrhenius plot of our data for cobalt diffusion shows a definite non-linearity. The activation energy and preexponential factor are 1.39 eV and 134 cm^2 sec^{-1} for temperatures above 320 °C, and 1.09 eV and 0.4 cm^2 sec^{-1} for the lower temperatures. The transition between the two temperature regions in the Arrhenius plot appears to occur over only a rather narrow range of temperature. A discussion of the nonlinear Arrhenius plots is deferred to a later part of this paper. Both sets of diffusion parameters could be typical of a vacancy mechanism. The belief that Co^{2+} does indeed diffuse substitutionally in AgCl over the entire temperature range is also corroborated by a low-temperature measurement at 196 °C which showed a downward curvature in the penetration plot. This is attributable to tracer contamination and is thus consistent with this mechanism; an interstitial mechanism would have produced a curvature of the opposite sign in the low-temperature plot.

Diffusion of nickel

Because of experimental problems resulting from tracer contamination, the difficulty of counting highly absorbed β rays, and the low tracer diffusivities in this case, reliable data could be obtained only over a short range of temperature (350–441 °C). The Arrhenius plot (Fig. 4; solid
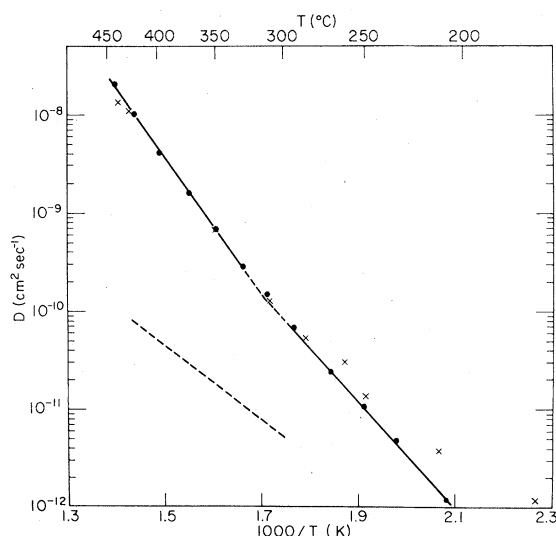

FIG. 5. Diffusion coefficient of Co^{2+} in AgCl, as a function of temperature. The solid circles refer to our data characterizing intrinsic diffusion; crosses refer to data obtained by Blackwell (Ref. 16). The results of Murin et al. (Ref. 17) are shown by a dashed line.

circles) is again curved, with an activation energy and a preexponential factor equal to 1.88 eV and 4.3×10^4 cm^2 sec^{-1} at higher temperatures and 1.48 eV and 40.1 cm^2 sec^{-1}, respectively, at lower temperatures. Because of the small temperature range of study in this case, these values are not as well-determined as for the other tracers, but they certainly imply that diffusion of Ni^{2+} proceeds by the vacancy mechanism.

Below 350 °C, the penetration plots were nonlinear (even though the intrinsic Frenkel defect concentration is still several hundred ppm), and the two diffusion coefficients measured from the "limiting" slopes are shown in Fig. 4 (open circles). A third diffusion coefficient (solid triangle) at the lowest temperature, 250 °C, was however determined from a nearly Gaussian penetration plot resulting from perhaps a total domination by extrinsic vacancies introduced by impurities in the tracer. These low-temperature data thus define only an upper limit, and of course it is doubtful that any quantitative significance can be attached to them. Nevertheless, the sign of the curvature of the penetration plots for these runs is informative in that it is again consistent with that expected for the diffusion of nickel by means of impurity-induced cation vacancies.

DISCUSSION

Nonlinearity in Arrhenius plots

The explanation of the nonlinearity evident in Fig. 5 for the diffusion of cobalt in AgCl, and in

Fig. 4 for the diffusion of nickel in AgCl is not clear. Similar nonlinearity was also observed earlier for the diffusion of zinc in AgCl.[18] It is well established that the defect concentration in AgCl rises above the expected $\exp(-G_f/2kT)$ at high temperatures, where G_f is the Gibbs free energy for formation of a separated Frenkel pair at moderate temperatures. The excess defect concentration is due only in part to Debye-Hückel electrostatic screening. There is also an anomalous decrease in the defect formation free energy at high temperatures,[19] perhaps a result of the anomalous thermal expansion and dielectric constant.[20] Thus one expects—and indeed observes— that the Arrhenius plot for diffusion of a monovalent substitutional solute such as Na$^+$ shows an upturn at temperatures above 300 °C.[21] One is therefore tempted to attribute the upward curvature of Fig. 5 to the same origin, since it begins at about the right temperature and turns up by approximately the right amount. It is not clear, however, that this interpretation is valid, in part because of uncertainties in the effects of Debye-Hückel screening on solute-vacancy complexes, but primarily because such an explanation predicts equivalent upturns for the diffusivities of *all* solutes. Thus, although the data for Ni^{2+} and Zn^{2+} do suggest such a curvature, no equivalent anomaly is apparent for V^{2+}, Cr^{2+}, or Fe^{2+}, nor was one observed previously[13] for Mn^{2+} or Cd^{2+} diffusing in AgCl. It is, of course, possible that some of the nonlinearity in Arrhenius plots is due to a perturbation of the low-temperature diffusivities by unknown impurities or other defects, but there is no evidence on this question. Thus, at present, this phenomenon is certainly not understood.

Crystal-field effects

The present experiments provide strong evidence that the first-row divalent transition-metal ions diffuse in silver chloride by means of the vacancy mechanism. It is instructive to compare their activation energies as one proceeds across the periodic table from V^{2+} to Ni^{2+}, a continuous series encompassing six ions. In making such a comparison, we use the activation energies obtained from the high-temperature region; these are the most accurately determined and are free of suspicion of any perturbation by impurities introduced into the crystal along with the tracers.

Table II summarizes these activation energies. Of particular interest is their systematic variation, from a very high value at vanadium through a minimum at manganese, then rising again through iron, cobalt, and nickel. Since each of these ions is doubly charged, such large effects cannot be associated with coulombic interactions. Also, this variation cannot be attributed to an effect of the changing radius of the solute ions. First, all of these solutes have ionic radii substantially less than that of the host Ag$^+$. Also, the decrease of ionic radius with increasing atomic number is not great, and occurs most rapidly at Mn^{2+}, where the diffusion activation energy is changing least rapidly. Finally, the activation energy rises again as one proceeds from Mn^{2+} to Ni^{2+}, while the ion radii continue to decrease from 0.80 to 0.69 Å. It thus appears that the systematic variation in diffusion activation energy is not related to the radii of the solute ions.

Noting that the activation energy is a minimum for the spherically symmetric Mn^{2+} (d^5 configuration), one is led to seek an interpretation in terms of the effects of the crystal field. As the jumping solute ion passes from its substitutional site to the interstitial saddle point (now adjacent to two otherwise vacant cation sites), the crystal-field splitting changes, and extra work must be done on the d-shell electrons. This extra work will be zero from the configurations d^5 (as for Mn^{2+}) and d^{10} (as for ions to the right of Ag$^+$, such as Zn^{2+}), but will be nonzero for all of the other solutes included in the present study. If the activation energy for the solute-vacancy exchange jump is de-

TABLE II. Relative activation energies for the diffusion of first-row transition-metal ions in AgCl.

Tracer	Configuration	Temperature range (°C)	Diffusion activation energy (eV)	$H_2^{solute} - H_2^{Mn^{2+}}$ (eV) Expt (± 0.03 eV)	Theory
V^{2+}	$3d^3$	352—441	2.08	0.90	0.96
Cr^{2+}	$3d^4$	325—440	1.25	0.06	0.11
Mn^{2+}	$3d^5$	249—420	1.18	0	0
Fe^{2+}	$3d^6$	274—442	1.26	0.07	0.03
Co^{2+}	$3d^7$	328—441	1.39	0.19	0.17
Ni^{2+}	$3d^8$	393—441	1.88	0.69	0.72
Zn^{2+}	$3d^{10}$	352—441	1.01	$\leqslant 0.18$	0

noted by H_2, then one wishes to compare the experimental values of $(H_2^{solute} - H_2^{Mn^{2+}})$ with the difference between the extra stabilization of nonspherical ions at the substitutional and interstitial sites. This difference can be calculated by means of crystal-field theory.

Now, the diffusion activation energy itself contains other components in addition to H_2, namely, one-half the formation energy of the Frenkel defect in the otherwise perfect lattice, plus the impurity-vacancy binding energy. In general, one might also anticipate a contribution from the temperature dependence of the correlation factor; that term, however, is negligible in the present experiments, because the solute jump frequencies are so much lower than that of the host cation that their correlation factors are all essentially unity.

The necessary values for the solute-vacancy binding energies for these ions have been obtained by Lieb[22] and Gerlach,[23] from a careful analysis of the temperature dependence of the ionic conductivity of appropriately doped AgCl crystals. Lieb's values of 0.247 eV (V^{2+}), 0.232 eV (Cr^{2+}), 0.239 eV (Fe^{2+}), 0.269 eV (Co^{2+}), and 0.236 eV (Ni^{2+}), along with Gerlach's 0.245 eV for Mn^{2+}, differ from one another by only several hundredths of an electron volt. They are all within the experimental error of 0.01 to 0.02 eV of the average value of 0.245 eV. For Zn^{2+}, however, the solute-vacancy binding is anomalously strong[23]—approximately 0.5 to 0.6 eV—as has been similarly found for this same ion in NaCl.[24] Thus, each desired value of $(H_2^{solute} - H_2^{Mn^{2+}})$ may be obtained from the difference between the total activation energies for solute diffusion, plus the difference in the two solute-vacancy binding energies. The experimental values thus obtained for $(H_2^{solute} - H_2^{Mn^{2+}})$ are given in Table II.

We now wish to estimate the crystal-field energies, for comparison with the experimental values of $(H_2^{solute} - H_2^{Mn^{2+}})$. We assume that, in the absence of crystal-field splittings at the the substitutional site and the saddle point (assumed to be the interstitial site), the solute migration energies of these $3d^n$ ions ($n = 3$ through 8) in AgCl would all be the same. This hypothetical activation energy may be identified with the value experimentally observed for the $d^5 Mn^{2+}$: The ground state for Mn^{2+} is ^6S, and thus cannot be split by a crystal field. For the other solutes, we treat the crystal-field splitting as a perturbation of the energy states of the shifted free ions. Under this assumption, an additional contribution to the migration energy arises from the difference between the lowering (beyond the center-of-gravity shift) of the electronic energy, by the crystal field, in the substitutional and the activated sites.

The crystalline field at the normal substitutional site has octahedral symmetry, but perturbed by the presence of the vacancy which, if the impurity is to diffuse, must be at the nearest-neighbor position. Optical absorption measurements[25] have determined the strength of the parameter Dq characterizing the octahedral field at the impurity. The fits to the optical data did not require taking the associated vacancy explicitly into account as a perturbing influence (this is not especially surprising since, in a point-ion model, the vacancy has only a 2% influence on Dq). Following this model, the relevant part of the crystal potential is

$$V_{substit} = 14\sqrt{\pi} Dq [Y_4^0 + \sqrt{5/14}(Y_4^4 + Y_4^{-4})] ,$$

where the Y_l^m denote the usual spherical harmonics describing the angular variation of the potential. This potential lowers the energy of the electronic ground state of the substitutional impurity ions by an amount denoted by ΔE_s in Table III. The quoted values of Dq are those of Koswig, Retter, and Ulrici,[25] measured at 20 K, and corrected to 400 °C by multiplying them by 0.90, the fifth power of the ratio of the lattice constants of AgCl at the two temperatures. The value of ΔE_s given for Co^{2+} is $6.57Dq$, rather than the conventional $6Dq$, due to the inclusion of F-P term mixing with an assumed separation of 11 925 cm^{-1}, as given by Sliker.[26] This partial contribution to the relative energy barrier (i.e., relative to that for Mn^{2+}) for migration among the $3d^n$ ion group is depicted in Fig. 6, if one takes equal to zero the parameter γ, which (as will be detailed below) measures the effect of the saddle-point field. It should be noted that, at this stage, even before
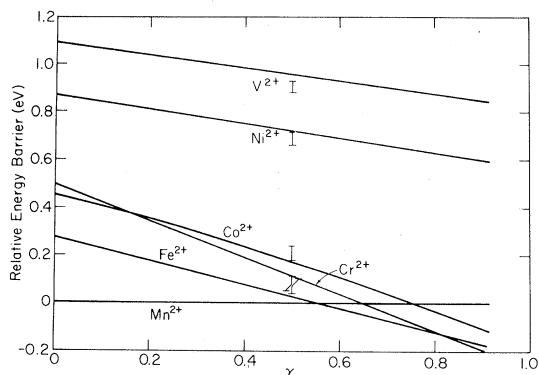

FIG. 6. Diffusion energy barrier, relative to Mn^{2+} vs the fitting parameter γ (defined in the text) which scales the strength of the potential felt by the diffusing ion at the activated position. The results for $\gamma = 0$ are those due solely to splittings at the substitutional site. A choice of $\gamma = 0.5$ gives good agreement with the experimental results noted for all five ions.

including effects of the crystal field at the saddle point, this contribution already puts V^{2+} at about 1.1 eV (relative to Mn^{2+}), Ni^{2+} close by at 0.87 eV, and Co^{2+}, Fe^{2+}, and Cr^{2+} all within 0.2 eV of one another and substantially below V^{2+} and Ni^{2+}.

The enhancement of the energy barrier due to the crystal-field splitting at the substitutional site is, however, only an upper limit to the final result, since the electronic ground-state energy of all the other solutes will also be below that of Mn^{2+} at the saddle point; that contribution will tend to decrease the magnitudes of the relative energy barrier. With the ion now placed at the interstitial saddle point, the crystal potential is more complicated. If it were simply the case of an interstitial ion with all adjacent sites normally occupied, there would be no crystal-field splitting in a point-ion model, by symmetry. There must exist, however, two adjacent positive ion vacancies, that from which the ion is jumping and the site into which it is about to jump. These vacancies are now much closer to the interstitial ion than was the vacancy which was successfully ignored when the ion occupied a substitutional site. Further, in contrast to the substitutional site, there is no experimental data to guide a crystal-field parametrization. A simple approach to a parametrization of the crystalline potential has been taken here by relating parameters, among themselves, by ratios which would hold if the crystal were actually composed of point ions; the remaining parameter, an overall strength, is related to the octahedral field, previously discussed, by the same point-ion ratio multiplied by an unknown constant. This constant represents the single, adjustable fitting parameter of the calculation. In this approach, the burden is being placed on the parameters obtained from the optical absorption data for the octahedral field. The fitting parameter would be unity if the ratio of the strengths of the potential in the saddle point and substitutional positions were the same as for point ions, and it would be small if the poten-

tial for the saddle point were weak. Explicitly, then,

$$V_{\text{activ}} = b_4^0 \left[Y_4^0 + \sqrt{5/14}\,(Y_4^4 + Y_4^{-4}) \right.$$
$$+ i\tfrac{9}{28}\sqrt{6/5}\,(\langle r^2 \rangle / \langle r^4 \rangle)R^2(Y_2^2 - Y_2^{-2})$$
$$\left. + i(\sqrt{10}/7)(Y_4^2 - Y_4^{-2}) \right],$$

with $b_4^0 = \tfrac{2}{9}(2/\sqrt{3})^5(14\sqrt{\pi}Dq)\gamma$. The quantity Dq has the values previously quoted, R is the anion-cation spacing for AgCl, $\langle r^2 \rangle$ and $\langle r^4 \rangle$ are the appropriate expectation values for the impurity ions (values from Abragam and Bleaney[27] were used), and finally, γ is the fitting parameter discussed above. Note that the term with the radial expectation values is large and that it explicitly depends on the diffusing ion.

This potential lowers the ground-state energy at the activated site by an amount denoted by ΔE_a in Table III. F-P mixing was considered and found to be relevant for V^{2+}, Co^{2+}, and Ni^{2+}. However, for values of γ between zero and unity the term mixing is non-negligible only for Co^{2+}, and causes the curvature observable in Fig. 6. Its effects in the interstitial and substitutional sites tend to cancel, and actually do cancel for $\gamma \simeq \tfrac{1}{2}$. Spin-orbit effects were neglected throughout, since they have been estimated to give a maximum effect of only a few hundredths of an electron volt.

We find that the experimental results can be best reproduced, in this calculation, for values of γ near 0.5, which is not unreasonable. The neglect of distortions associated with the impurity ion, along with the very nature of the host crystal, which has valence bands which are hybrids of Ag^+ d states and Cl^- p states, precludes a more exact simple calculation of the crystal field in the activated configuration; hence, it is difficult to justify our parametrization in detail. The agreement of the calculation with experiment, however, is surprisingly good. First, the qualitative predictions of the model, that the relative energy barriers will be substantially larger for V^{2+} and Ni^{2+}

TABLE III. Calculated lowering of the ground-state energy of ions in AgCl for the substitutional and activated sites.

Ion	Configuration	Dq (cm^{-1})	$\Delta E_s/Dq$	$\Delta E_a/Dq$
V^{2+}	$3d^3$	734	12	2.82γ
Cr^{2+}	$3d^4$	666	6	9.30γ
Mn^{2+}	$3d^5$	585	0	0
Fe^{2+}	$3d^6$	558	4	7.21γ
Co^{2+}	$3d^7$	554	6.57	$7.04\gamma + \dfrac{63.15\gamma^2}{21.53 + 7.04\gamma}$
Ni^{2+}	$3d^8$	585	12	4.11γ

(whose ordering and difference is nearly independent of the value chosen for γ) than for the remaining ions seem sufficient to uphold the interpretation. Second, quantitative comparison of the calculated ΔH's (Table II, last column) with the experimental values shows that, with only the single adjustable parameter γ, excellent agreement can be obtained for the entire set of solutes.

Hence, it would seem that the present work establishes reasonably firmly that the electronic structure and its interaction with the crystal field is the origin of the systematic differences among the activation energies of the $3d^n$ ion group.

ACKNOWLEDGMENTS

[1] D. Lazarus, Phys. Rev. 93, 973 (1954).
[2] A. LeClaire, Philos. Mag. 7, 141 (1962).
[3] L. Slifkin, Semicond. Insul. 3, 393 (1978).
[4] P. Varotsos and D. Miliotis, J. Phys. Chem. Solids 35, 927 (1974).
[5] M. Cox, B. McEnaney, and V. Scott, Philos. Mag. 26, 839 (1972); Nature (London), Phys. Sci. 237, 140 (1972).
[6] A. Batra, J. Hernandez, and L. Slifkin, Phys. Rev. Lett. 36, 876 (1976).
[7] A. Batra and L. Slifkin, J. Phys. Chem. Solids 30, 1315 (1969).
[8] S. Cheema and M. Smith, J. Phys. C 2, 1751 (1969).
[9] W. Ulrici, Phys. Status Solidi 27, 333 (1968).
[10] I. Kunze and P. Müller, Phys. Status Solidi 33, 91 (1969).
[11] P. Süptitz, Phys. Status Solidi 7, 653 (1964).
[12] A. Batra, A. Laskar, and L. Slifkin, J. Phys. Chem. Solids 30, 2053 (1969).
[13] A. Batra and L. Slifkin, J. Phys. C 8, 2911 (1975).
[14] D. Foster and A. Laskar, Phys. Status Solidi A 29, 167 (1975); also, D. Foster, M. S. thesis, Clemson University, 1972 (unpublished).
[15] J. Mitchell and D. Lazarus, Phys. Rev. B 12, 734 (1975).

[16] R. Blackwell, M. S. thesis, Clemson University, 1971 (unpublished).
[17] A. Murin, B. Luré, P. Seregin, and N. Cherezov, Fiz. Tverd. Tela. (Leningrad) 8, 3291 (1966) [Sov. Phys.—Solid State 8, 2632 (1967)].
[18] A. Batra and L. Slifkin, Phys. Status Solidi A 19, 171 (1973).
[19] J. Aboagye and R. Friauf, Phys. Rev. B 11, 1654 (1975).
[20] P. Varotsos and K. Alexopoulos, J. Phys. Chem. Solids 39, 759 (1978).
[21] A. Batra and L. Slifkin, Phys. Rev. B 12, 3473 (1975).
[22] R. Lieb, Ph.D. thesis, University of North Carolina, 1976 (unpublished).
[23] J. Gerlach, Ph.D. thesis, University of North Carolina, 1974 (unpublished).
[24] S. Rothman, L. Barr, L. Rowe, and P. Selwood, Philos. Mag. 14, 501 (1966).
[25] H. D. Koswig, W. Retter, and W. Ulrici, Phys. Status Solidi B 51, 123 (1972).
[26] T. R. Sliker, Phys. Rev. 130, 1749 (1963).
[27] A. Abragam and B. Bleaney, Electron Paramagnetic Resonance of Transition Ions (Clarendon, Oxford, 1970), p. 399.